ANALYSIS OF WAVE INFLUENCE ON STEAM CONDENSATION WITH NON-CONDENSABLE GASES USING CFD

Xianmao Wang, Huajian Chang
Institute of Nuclear and New Energy Technology
Tsinghua University
Beijing 100084, China
Wangxianmao123@163.com; changhj@mail.tsinghua.edu.cn

Liyong Han
State Nuclear Power Technology R&D Center
Beijing 100190, China
hanliyong@snptrd.com

ABSTRACT

Steam condensation can play an important role during heat removal processes after a postulated accident in a nuclear power plant. However, due to the presence of non-condensable gases such as air and hydrogen in the containment, the rate of heat transfer can decrease dramatically. Past work by researchers all around the world have studied the effects of steam condensation in the presence of non-condensable gases, both experimentally and by phenomenological modeling. In recent years, computational fluid dynamics (CFD) methods have been used to study this phenomena and reasonable results have been obtained. However, these CFD simulations have normally neglected the falling film to reduce the complexity of the problem. In this study, a CFD approach is applied to simulate the steam condensation process with a falling film. The volume of fluid (VOF)method is used to model the two-phase flow. Surface tension and shear stress are considered. Condensation mass transfer is added as a source term in the model. The velocity of the gas mixture is adjusted to simulate different condensation situations. The influence of the waviness structure of the falling film on gas phase is analyzed.

KEYWORDS
CFD, Condensation, Falling Film, Wave

1. INTRODUCTION

Film steam condensation in presence of non-condensable gases has been widely studied both experimentally and theoretically. Almost all of the parameters that effect steam condensation rate have been studied, among which mass fraction of non-condensable gases is found to be the most important one. Even a small amount of non-condensable gases can reduce condensation rate dramatically. A large amount of experiments that focus on steam condensation have confirmed this. That is also why the mass fraction of non-condensable gases is treated as the major variable in many experimental correlations. For theoretical study, since it is not easy to solve all the field equations for steam condensation with non-condensable gases, the analogy between heat and mass transfer becomes a more common approach for engineering application.

In recent years, computational fluid dynamic (CFD) is becoming a more popular approach in studying film steam condensation in presence of non-condensable gases because of its convenience and less cost. Kljenak and Babic(2008)[1] use CFX4 to model steam condensation with non-condensable gases in the containment. The condensation rate is calculated according to Uchida et al. (1965) experimental correlation. The calculation results are compared with experimental data from TOSQAN and ThAI facilities and good agreement is acquired. Dehbi[2] and Ambronisi[3]applied stagnant film mass transfer theory to calculate the condensation rate. In this approach very fine meshes are required in the near wall region. The computational results are also quite satisfactory. What is in common is that all these CFD models mentioned above treat steam condensation in a gas mixture as single-phase flow and the mass loss due to condensation are added as source terms in the near-wall cells. Almost all these CFD model neglected the falling film to reduce the complexity of the problem.

However, it has been found by some researchers that falling film has important influence on steam condensation not only due to liquid thermal resistance and interface shear stress, but also due to wavy structures of the falling film. Kim et al.(1990) [4]considered wavy interface of the falling film in their study as a rough wall surface and they found that wavy structures can enhance the condensation heat transfer around 10%. Park and Kim(1997)[5] studied wave influence on condensation experimentally. They found that when the film Reynolds number is large enough, wavy structures can enhance condensation mass transfer. However, in their research, when film Reynolds number is below 350, wave influence is not considered. On the other hand, in the experiment conducted by Karapantsios et al.(199)[6], they found wave structures have slightly negative effect on condensation rate. One thing should be mentioned is that in their experiments, gas mixture was stagnant, which is different from the cases we normally consider. As a result, the influence of the wavy structures on steam condensation is still unclear.

In the current work, the effect of wavy interface of the falling film on steam condensation is studied based on CFD. The volume of fluid (VOF)method is used to model the two-phase flow. Surface tension and shear stress are considered. A phase change model is implemented as well. The film Reynolds number, gas velocity and wavy structure are changed to study the influence of the waviness structure of the falling film on gas phase.

2. CFD MODEL

The two-dimensional transient-state simulations are performed with FLUENT. The VOF method is applied to track the interface of liquid and gas. The Geo-Reconstruct scheme is used in together with the explicit scheme for time discretization. Reynolds averaged Navier-Stokes (RANS) turbulent model is applied to simulate the turbulence. A Phase change model is implemented by user-defined function(UDF). An overview of the general features of the applied CFD model is given in Table I.

Table I. General Features of The CFD Model

Solver	Pressure-based segregated
Formulation	Transient
Algorithm	PISO
Turbulence	RANS
VOF scheme	Geo-Reconstruct
Pressure interpolation	PRESTO!

2.1. VOF Method

The VOF method is a multiphase model, which can be used to track the interface of immiscible fluids. For a two-phase mixture, interface tracking is accomplished by the solution of a transport equation for the volume fraction of the second phase. The volume fractions of all phases sum to unity in each control volume[7].

$$\frac{\partial \alpha_2}{\partial t} + \nabla \cdot \left(\alpha_2 \vec{v} \right) = S \tag{1}$$

$$\alpha_1 + \alpha_2 = 1 \tag{2}$$

The properties of the two-phase mixture such as density and viscosity are determined by an arithmetic mean of the presence of the component phases in each control volume:

$$\varphi = \alpha_2 \varphi_2 + \left(1 - \alpha_2\right) \varphi_1 \tag{3}$$

The method solves a single set of momentum equations. The resulting velocity field is shared among the phases.

$$\left(\rho \vec{v} \right) + \nabla \cdot \left(\rho \vec{v} \vec{v} \right) = -\nabla p + \nabla \left[\mu \left(\nabla \vec{v} + \nabla \vec{v}^{T} \right) \right] + \rho \vec{g} + \overrightarrow{F_\sigma} \tag{4}$$

To account for the effect of surface tension, the Continuum Surface Force(CSF) model proposed by Brackbill et al.[8] is used.

$$\kappa = \nabla \cdot \frac{\nabla \alpha_2}{\left| \nabla \alpha_2 \right|} \tag{5}$$

$$\overrightarrow{F_\sigma} = \sigma_{21} \frac{\rho \kappa \nabla \alpha_2}{0.5\left(\rho_1 + \rho_2 \right)} \tag{6}$$

Where κ is the surface curvature and σ_{12} is the surface tension.

The energy equation is also solved among the phases.

$$\frac{\partial}{\partial t}\left(\rho E \right) + \nabla \cdot \left[\vec{v} \left(\rho E + p \right) \right] = \nabla \cdot \left(k_{eff} \nabla T \right) + hS \tag{7}$$

Where k_{eff} is the effective thermal conductivity and the last term is the energy source due to phase change.

A single set of scalar equation for species transport is solved as well. Also, the turbulence variables are shared by the phases throughout the field.

Wavy structure is one of the most important features of falling film. In this study, wave is produced by a perturbation with a fixed frequency which is introduced at the water inlet. The water inlet velocity is given by:

$$u = \left(1 + \varepsilon \sin(2\pi f t)\right)\bar{u} \tag{8}$$

Where f is the frequency and ε is the magnitude.

2.2. Turbulence Model

Previous researches have shown that the transition Reynolds number for falling film from laminar to turbulent is around 1000~2000. In the situation of steam condensation in the containment, the Reynolds number of the condensing film can hardly reach 1000. Thus, the falling film can be considered as laminar flow while gas phase in the containment should be treated as turbulent flow. However, the VOF method only solves one set of turbulent equation. To overcome the problem, a modified equation is used to compute turbulent viscosity.

We choose the SST turbulence model because it can directly solve two-layer model near the wall if the near-wall mesh is fine enough. In the current study, the turbulent viscosity is computed as follows:

$$\mu_t = \alpha \rho_v \frac{k}{\omega} \tag{9}$$

Since turbulent viscosity is a function of volume fraction of the first phase, in the liquid phase the turbulent viscosity is zero. In this way, turbulence production is suppressed in the liquid phase[9]. The damping factor for turbulent viscosity in SST model is not incorporated because it has little influence on the calculation in the current study.

2.3. Mass Transfer Model

The mass transfer model is based on diffusion through stagnant film mass transfer mechanism and is accomplished by adding source term to continuity and species equations[10].

The source term is given by:

$$S = \frac{D_{ij}\rho_v}{1 - W_i} \nabla W_i \,|_{\mathrm{i}} \cdot A \tag{10}$$

A is the normal interfacial mass transfer area, which is given by:

$$A = V_{cell} \nabla \alpha \tag{11}$$

In the interface cells which gas volume fraction is between zero and one, the source terms are applied and the equilibrium mass fraction is assigned by using the concept of internal boundary condition[11]. The equilibrium mass fraction is determined from Dalton’s Law of partial pressure at saturated pressure near the interface.

$$W_{eq} = \frac{x_i M_i}{x_i M_i + (1 - x_i) M_v} \tag{12}$$

2.4. Computational Mesh

Structured two-dimensional grids are constructed. The computational domain is shown in Figure 1. In order to fully resolve the viscous sublayers in the near wall region, the dimensionless length scale in the first cell next to the wall is kept lower than 1. The computational domain is divided into two regions: liquid-phase dominated region and gas-phase dominated region. In the liquid-phase dominated region, the cells in the transversal direction with respect to main flow is 0.00005m while the cells in the parallel direction is 0.00025m. In the gas-phase dominated region, the mesh is much coarser in the core region while in the near-wall region, the mesh is still rather fine.

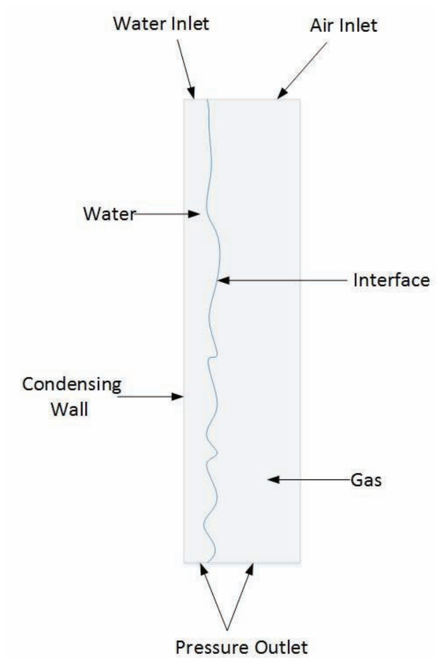

Figure 1.Computational Domain

3. VALIDATION

The computational model is validated against the COPAIN condensation experiment which was conducted to study steam condensation in presence of non-condensable gases[12]. The test section of COPAIN facility consists of a rectangular channel of depth 0.5 m in which a vertical condensing plate of 2m long and 0.6 m wide is placed. Coolant water flows at the back of the plate to provide a uniform temperature. All walls except the condensing plate are insulated. Gas temperature, velocity and mass fraction and the heat flux through the plate were recorded.

In this study, all four cases provided in Dehbi's[2] paper chosen from COPAIN are compared with CFD prediction, shown in Table II. Since capturing the detail structure of the falling film needs considerable amount of control volumes, it is very time-consuming to simulate the whole flow channel. Thus, only the fully developed section is simulated with two-phase computational model and the inlet boundary of vapor flow of the fully developed section is obtained from single-phase simulations with condensation model proposed by Ambrosini[3].

The single-phase condensation model is also based on diffusion through stagnant film mass transfer mechanism. The difference is that this model neglects condensing film and only the gas phase is considered. The mass and species source terms due to condensation are add in the cell next to the condensing wall. The single-phase condensation model has already been validated by Ambrosini[3] and Houkoma[13]. The CFD prediction results are satisfactory.

In the work, single-phase condensation is used to simulate the beginning 1.8m of the condensing plate. The simulate results have good agreement with experimental data. After that, The results of these simulations are then used to set the inlet boundary conditions for the x,y velocity component , the turbulent kinetic energy and the turbulent specific dissipation rate and temperature and gas mass fraction, as it's shown in Fig.2. The velocity of the inlet water is calculated according the sum of the condensation rate along 1.8m of the condensing plate.

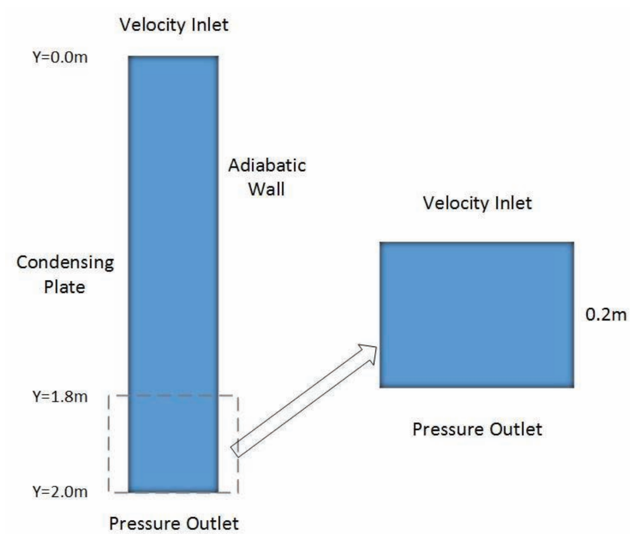

Figure 2.Test Section of COPAIN

Table II. Four Cases from COPAIN

Test	Inlet velocity(m/s)	Absolute pressure(bar)	Inlet temperature(K)	Wall temperature(K)	Air mass fraction
P0441	3.0	1.02	353.2	307.4	0.767
P0443	1.0	1.02	352.3	300.1	0.772
P0444	0.5	1.02	351.5	299.7	0.773
P0344	0.3	1.21	344.4	322.0	0.864

The local condensation heat transfer rates are listed in Table III. From the table we can see that the computational results given by single-phase model and current model are rather close to each other. Both models give quite satisfactory results compared to the experiment. The difference between the experimental data and calculation result is lower than 25%. The condensation heat fluxes calculated by current model are a little higher than that calculated by single-phase model, however, we cannot simply conclude that condensing film tends to enhance the condensation process since considerable amount of features of the two models are different.

Table III. CFD Validation Results

Test	$q_{experiments}$ (W/m²)	$q_{single\text{-}phase\ model}$ (W/m²)	$q_{current\ model}$ (W/m²)
P0441	4642	4928	5099
P0443	2693	2578	2608
P0444	2609	2412	2587
P0344	992	753	774

4. RESULTS AND DISSCUSION

The water flow rate, wave frequency and air velocity are adjusted to investigate the influence of falling film on condensation. The range of film Reynolds number is from 36 to 312. Gas velocity ranges from 4m/s to 12 m/s. Two wave frequencies, 12.7 and 25.5 are chosen. The wavy cases are compared with cases which have flat film. After calculating considerable amount of cases, we did not find distinct enhancement of the mass transfer due to wavy structure. One typical case is shown below in figure 3. The film Reynolds number, the gas velocity and the wave frequency are 312, 4m/s, and 25.5, respectively. From the comparison of local condensation rate we can find that at the peak of the wave crest, the condensation rate is higher than that of flat film. However the condensation rate is quite lower at the bottom of the wave front. As a result, the enhancement of the mass transfer at the peak of the wave is compensated. Almost all cases show the similar trend. Figure 4 shows the velocity vectors near the interface, which is colored by the volume fraction of phase one. As we can observe, near the wave crest, both liquid phase and gas phase have larger velocities than that of the wave tail. Non-condensable gas around the wave crest tends to be blow away by the larger velocity, while at the wave tail, non-condensable gas tends to accumulate since the velocity of the gas phase is rather small.

Table IV. Computational Results

Gas velocity (m/s)	Frequency of the wave	Liquid Reynolds number	Magnitude of the wave (mm)	Condensation rate (Kg/s)
4	Flat	312	None	0.000559
4	Flat	120	None	0.000537
4	12.7	312	0.43	0.000532
4	12.7	120	0.31	0.000519
4	25.5	312	0.34	0.000534
4	25.5	120	0.21	0.000514
12	Flat	312	None	0.001168
12	Flat	120	None	0.001137
12	25.5	312	0.28	0.001141
12	25.5	120	0.19	0.001128

The frequency of the wavy structure does not show distinct influence on condensation rate as well, which can be found from cases listed in Table IV, though the magnitude of the wave decreases when the frequency of the wave increases. The reason of this negligible effect of wavy interface on condensation rate may be that the magnitude of the wave is not high enough to alter the non-condensable gas boundary layer.

Falling film Reynolds number has a little positive effect on condensation rate, which also can be seen in Table IV. The small increase of condensation rate along with the increase of film Reynolds number cannot be simply ascribed to the enhancement of wavy magnitude, since the flat film also shows the similar trend.

Since the film Reynolds number in the current study is limited below 320, the magnitude of the wave is rather small. Thus, more calculations with larger film Reynolds number are still necessary.

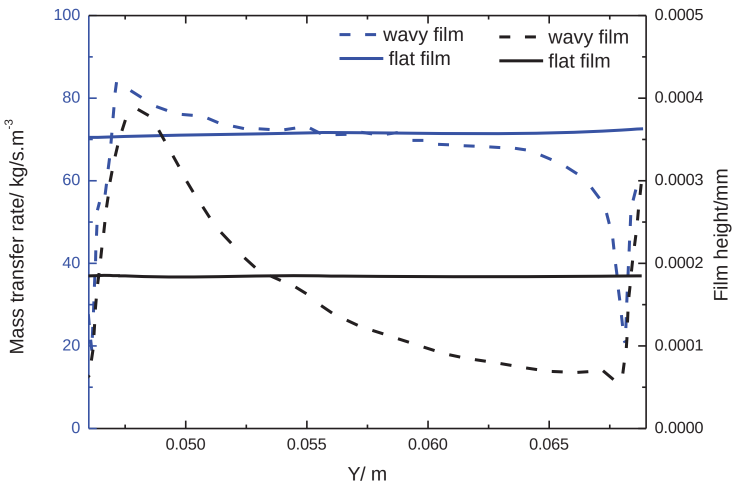

Figure 3. Comparison of Film Height and Mass flow Rate of Wavy Film and Flat Film Along the Condensing Wall

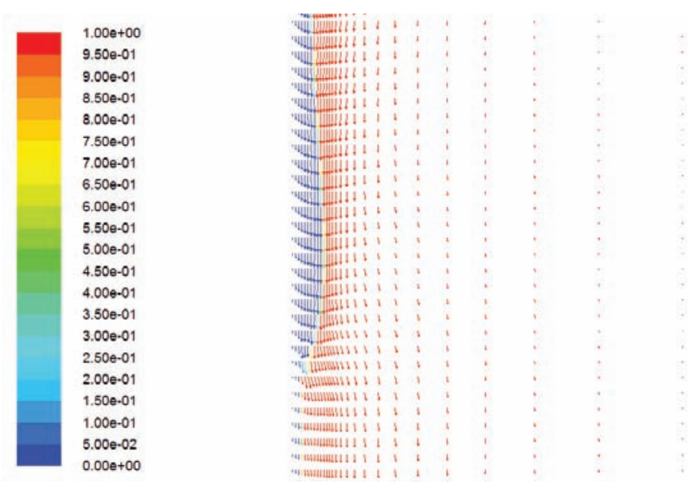

Figure 4. Velocity Vectors Colored by Volume Fraction of Phase One

5. CONCLUSIONS

In the paper, a new condensation model based on VOF method is built to investigate the influence of wavy structures on condensation rate. The model is validated against COPAIN tests. The effect of wavy interface of the falling film on steam condensation is studied by changing the film Reynolds number, gas velocity and film wave frequency. The enhancement of condensation rate due to wavy interface is found to be negligible when film Reynolds number is less than 350. However, the local condensation rate is different due to the wavy interface. At the peak of the wave crest, the condensation rate is higher than that of the flat film. However the condensation rate is quite lower at the bottom of the wave front. The magnitude of the wave decreases when the frequency of the wave increases, but the influence of wave frequency is also not distinct in the current study. Falling film Reynolds number has a little positive effect on condensation rate, but we cannot easily draw the conclusion that the small increase of condensation rate is because of the enhancement of wavy magnitude, since the flat film also shows this similar trend. Further studies are still needed to have a more comprehensive understanding of the wavy influence on steam condensation process.

NOMENCLATURE

A	area of the cell on the wall(m^2)
D	diffusion coefficient (m^2/s)
Re	Reynolds number
S	source term
T	temperature(K)
V	cell volume(m^3)
W	mass fraction
f	frequency
x	mole fraction

Greek symbols

α	volume fraction
ω	specific dissipation rate($1/s$)
ε	magnitude
ρ	density(kg/m^3)

Subscripts

v	gas
i	interface

ACKNOWLEDGMENTS

This work is supported by the scholarship from China Scholarship Council (CSC).

REFERENCES

1. M.Babic, I.Kljenak, B.Mavko, “Prediction of light gas distribution in experimental containment facilities using the CFX4 code,” *Nucl. Eng. Des.*, **238**, pp.538-550 (2008).

2. A.Dehbi , F.Janasz , B.Bell, “Prediction of steam condensation in the presence of non-condensable gases using a CFD-based approach,” *Nucl. Eng. Des.*, **258**, pp.199-210 (2013).
3. W.Ambrosini , N.Forgione, F.Oriolo, “Experiments and CFD analyses on condensation heat transfer in a square cross section channel,” *Proceedings of the 11th International Topical Meeting on Nuclear ReactorThermal-Hydraulics (NURETH-11)*, France, 2005.
4. M. H.Kim, and M. L.Corradini, “Modeling of condensation heat transfer in a reactor containment,” *Nucl. Eng. Design*, **118**, pp.193-212 (1990).
5. S.K .Park, M.H. Kim, “Effects of wavy interface on steam-air condensation on a vertical surface,” *Int. J.Multiphase Flow*, **23**, pp.1031-1042 (1997).
6. T.D.Karapantsios, M.Kostoglou, and A.J. Karabelas, “Local Condensation Rates of Steam-air Mixtur es in Direct Contact with a Falling Liquid Film,” *Int.J.Heat Mass Transfer.*, **38**(5), pp.779-794(1995).
7. ANSYS, Fluent 14.5, Theory Guide, ANSYS, Inc.
8. J. U.Brackbill, D. B.Kothe, and C. A.Zemach, “Continuum Method for Modeling Surface Tension,” *Journal of Computational Physics*, **100**, pp.335–354 (1992).
9. S.Bortolin, E.D. Riva, D.D.Col, “Condensation in a Square Minichannel: Application of the VOF Method,” *Heat Transfer Engineering*, **35**(2), pp.193-203(2013).
10. R.Banerjee, “A numerical study of combined heat and mass transfer in an inclined channel using the VOF multiphase model,” *Numerical Heat Transfer Part A*, **52** (2), pp.163-183 (2007).
11. S.V.Patankar, *Numerical Heat Transfer and Fluid Flow*, Taylor and Francis, Philadelphia(1980).
12. X.Cheng, P.Bazin, et al., “Experimental Data Base for Containment Thermalhydraulic Analysis,” *Nucl. Eng. Des.*, **204**,pp:267-284(2001).
13. M.Houkema, N.B.Siccama, “Validation of the CFX4 CFD code for containment thermal-hydraulics,” *Nucl. Eng. Des.*, **238**.pp.590-599 (2008).